Interfacial properties of amphipathic β strand consensus peptides of apolipoprotein B at oil/water interfaces

Libo Wang and Donald M. Small[1]

Department of Physiology and Biophysics, Boston University School of Medicine, Boston, MA 02118

Abstract **The region between residues 968 and 1882 of apolipoprotein B (apoB-21 to apoB-41) is rich in amphipathic β strands (AβSs) and promotes the assembly of primordial triacylglyceride (TAG)-rich lipoproteins. To understand the importance of AβS in recruiting TAG, the interfacial properties of two AβS consensus peptides, P12 and P27, were studied at dodecane/water (DD/W) and triolein/water (TO/W) interfaces. P12 (acetyl-LSLSLNADLRLK-amide) and P27 (acetyl-LSLSLNADLRLK*NGN*LSLSLNADLRLK-amide), when added into the aqueous phase surrounding a suspended oil drop (dodecane or triolein), decreased the interfacial tension (γ) in a concentration-dependent manner. At the DD/W interface, 1×10^{-5} M P12 decreased γ to ∼20 mN/m and 6.6×10^{-6} M P27 decreased γ to ∼13 mN/m. At the TO/W interface, 1.5×10^{-5} M P12 decreased γ to ∼14 mN/m and 9.0×10^{-6} M P27 decreased γ to ∼12 mN/m. The surface area of both peptides was between 11.2 and 15.1 Å^2 per residue, consistent with β sheets lying flat on DD/W and TO/W interfaces. P12 and P27 are almost purely elastic on DD/W, TO/W, and air/water interfaces. When P12 and P27 were compressed beyond the equilibrium γ to as low as 4 mN/m, they could not be readily desorbed from either interface. These properties probably help in assembling nascent TAG-rich lipoproteins, and AβS may anchor apoB to β lipoproteins.**—Wang, L., and D. M. Small. **Interfacial properties of amphipathic β strand consensus peptides of apolipoprotein B at oil/water interfaces.** ***J. Lipid Res.*** **2004.** 45: **1704–1715.**

Supplementary key words dodecane/water interface • triolein/water interface • air/water interface • low density lipoprotein

Apolipoprotein B (apoB) plays an obligate part in the process of the assembly and secretion of nascent VLDLs from the liver and of nascent chylomicrons from intestinal epithelial cells. It participates in the assembly of lipids, including phosphatidylcholine (PC), triacylglycerol (TAG), and probably cholesteryl esters and free cholesterol, into a nascent particle that is then secreted into the extracellular space and ultimately enters the blood. Once in blood plasma, nascent VLDLs are acted on by lipoprotein lipase (1) and converted to intermediate density lipoproteins, which are partly taken up by the liver and partly further converted by hepatic lipase into LDLs (2) after most of the TAG is removed. LDL then circulates in the plasma to be taken up by various organs that require it for the formation of hormones, bile acids, and new cellular membranous components. Excessive LDL accelerates the formation of atherosclerosis and its sequelae. Dietary fat enters the circulation through the formation and secretion of chylomicrons in the intestine. In the capillaries of adipose tissue and muscle, chylomicrons are acted on by lipoprotein lipase, which hydrolyzes much of their TAG and rapidly converts them to chylomicron core remnants. These remnants, enriched in apoE, are taken up rapidly by the liver and their contents recycled into the hepatic pool of lipids. During secretion and after the nascent particles enter the plasma, different soluble, exchangeable apolipoproteins bind to the surfaces and act as cofactors for a number of enzymes, including lipoprotein lipase, hepatic lipase, and LCAT. These small apolipoproteins are able to exchange off of chylomicrons and VLDL as the lipoprotein changes its size, composition, and surface pressure during lipolysis (1). However, apoB-100 and apoB-48 remain bound to the core part of the original nascent particle, which ends up as either chylomicron core remnants or LDLs and does not exchange between particles. In a recent review, Segrest and coworkers (3) suggested that apoB is not exchangeable because tightly bound regions of amphipathic β sheet prevent it coming off of VLDL during metabolism. This paper looks at a consensus sequence derived from the first β sheet region of apoB between apoB-21 and apoB-41 and its interaction with hydrocar-

Manuscript received 16 March 2004, in revised form 2 June 2004, and in re-revised form 16 June 2004.

Published, JLR Papers in Press, July 1, 2004.
DOI 10.1194/jlr.M400106-JLR200

Abbreviations: AβS, amphipathic β strand; apoB, apolipoprotein B; A/W, air/water; CSP, consensus sequence peptide, an amphipathic α helix consensus peptide derived from the water-soluble human apolipoproteins apoA-I, apoA-IV, and apoE and with the sequence (PLAEELRARLRAQLEELRERLG)2-NH_2; DD/W, dodecane/water; GIXD, grazing incidence X-ray diffraction, HFIP, 1,1,1,3,3,3-hexafluoro-2-propanol; MTP, microsomal triglyceride transfer protein; PC, phosphatidylcholine; TAG, triacylglycerol; TO/W, triolein/water.

[1] To whom correspondence should be addressed.
e-mail: dmsmall@bu.edu

bon and triolein surfaces and finds that it can be compressed to high pressures and is very difficult to force off the interface once it is bound.

In the past, several groups using C-terminal truncations of apoB have shown that the buoyant density of nascent lipoprotein secreted from cell cultures decreases as the N-terminal length of apoB is increased (3–6). Carraway et al. (7), using C-127 cells transfected with apoB of different length N-terminal regions and careful lipid, density, and cryoEM analysis, showed that significant TAG recruitment started between apoB-29 and apoB-32. These cells make no other apolipoproteins (8, 9) and were reported to have no detectable microsomal triglyceride transfer protein (MTP) activity (10). Recently, a very small amount of MTP mRNA and protein was found in C-127 cells, but far less than in hepatic cell lines (11). Carraway et al. (7) found in C-127 cells that ~70 molecules of surface lipids (mainly phospholipids) are recruited to apoB-29 (the N-terminal 29% of apoB), but very little TAG (~6 molecules) is secreted in apoB-29 lipoproteins. However, as the N-terminal region lengthens, more TAG is recruited. Between apoB-32 and apoB-41 there is a linear increase in the total number of TAG molecules, from ~15 in apoB-32 to almost 200 in apoB-41. Cryoelectron microscopy images of apoB-37 and apoB-41 particles show quasi-spherical particles with an electron-lucent center consistent with a neutral lipid core (7). Thus, it appears that the amphipathic β strands (AβSs) between apoB-32 and apoB-41 are responsible for most of the recruitment of TAG in MTP-poor C-127 cells. However, in COS cells transfected with high levels of MTP and truncated apoB, Shelness et al. (12) showed that phospholipid and TAG recruitment appears to begin at approximately apoB-19.5 to apoB-20.1, with increasing amounts of lipid being added as the sequence lengthens. Thus, β sheet regions throughout the apoB-20 to apoB-41 region are important for lipid recruitment, which may start at approximately apoB-20 if high MTP is expressed (12) but later in the sequence if MTP is relatively deficient (7).

Computer modeling along the amino acid sequence of apoB-100 has identified five regions: *1*) an α/β mixed region between the N-termini of apoB and apoB-20; *2*) a β sheet-rich region between apoB-20 and apoB-42; *3*) an α helix-rich region between apoB-42 and apoB-55; *4*) a second β sheet-rich region (apoB-55 to apoB-90); and *5*) an α helix-rich C-terminal region (3, 13, 14). The N-terminal domain up to apoB-20.5 contains α helices and amphipathic β sheets and is essential for the secretion of apoB (3, 15–17). It has high homology to MTP and lipovitellins (18–20). The X-ray crystal structure of lamprey lipovitellin (21) suggests that this homologous region of apoB could form part of a "lipid pocket" domain (18, 19), but homology to apoB stops at apoB-20.5 (18), and MTP-poor C-127 cells secreting apoB-17 (18) and apoB-20.5 (M. Carraway and H. Herscovitz, personal communication) are secreted with only a very small amount of surface lipids. Small and Atkinson (22) predicted that the region between apoB-21 and apoB-41 contained at least 41 AβSs of 11 amino acids or longer. They suggested that AβSs should have a strong lipid binding capacity and that their direct binding to TAG was energetically favored (22). Indeed, this β sheet region of apoB was shown to be involved in lipid binding to form VLDL-like particles (23) in hybrid apoB constructs (24) in chimeras between apoA-I and apoB (23) and directly to TAG (7).

Using a multialgorithmic approach to predict amphipathic secondary structure (13, 25, 26), we found that greater than 60% of the amino acids in the domain apoB-21 to apoB-41 were in amphipathic β sheets (22). These predictions are consistent with the recent model of LDL presented by Segrest et al. (3). Between apoB-20.5 and apoB-41, at least two significant putative amphipathic helical regions were identified, one at apoB-21 and the second cluster of three amphipathic α helices centered at apoB-26.7. Probably both α and β domains in the region between apoB-21 and apoB-29 are responsible for surface lipid recruitment to nascent apoB-29 particles in MTP-poor C-127 cells (7), but they might be responsible for binding PC and TAG in high MTP-expressing COS cells (12).

To specifically define the amphipathic β sheet regions between apoB-32 and apoB-41, which recruit TAG in C-127 cells, we used the same criteria we used previously to define β strands in apoB-21 to apoB-41 (13, 22, 25, 26). A minimum window of plus or minus five amino acids was slid along the sequence to identify AβSs of 11 residues or longer (13). The cutoff at 11 amino acids was used because it represents a strand of adequate length to span across a membrane and also fit within the estimated width of apo-B of 40–60 Å on LDL (27). The criteria to identify the AβSs were as follows: *1*) it must have a strongly hydrophobic face; *2*) only one strongly polar amino acid (N, Q, or H) and no charged residues (D, E, K, or R) were allowed in the hydrophobic face; and *3*) only one hydrophobic amino acid was allowed in the hydrophilic face. Using these criteria, 41 AβSs of 11–15 residues were identified between amino acids 968 and 1,882 (apoB-21 to apoB-41). Between residues 1,456 and 1,882 (apoB-32 to apoB-41), 24 AβSs were identified. These putative β strands account for 267 of the 425 residues (63%) between apoB-32 and apoB-41. These strands are aligned and shown in **Fig. 1**. Several shorter strands have also been predicted in this region by Nolte (13) and Segrest et al. (3) but are not included in this figure or in the calculations of the consensus sequence. The average change in free energy on transferring each residue from water to oil ($\Delta G_{W\rightarrow O}$) using a standard Goldman-Engleman-Steitz (GES) scale (28, 29) was averaged for each amino acid column (1–12) and tabulated at bottom. Every other column shows a strong negative $\Delta G_{W\rightarrow O}$, indicating the hydrophobic nature of the residues (columns with odd numbers). The even-numbered columns are hydrophilic, with an unfavorable $(+)\Delta G_{W\rightarrow O}$. Thus, the putative β strands are highly amphipathic with a hydrophobic face, having an average $\Delta G_{W\rightarrow O}$ of −2.03 kcal/mol residue, and the opposing face is quite hydrophilic (ΔG = 4.18 kcal/mol residue).

From the aligned sequence in Fig. 1, we estimated a 12 amino acid consensus sequence. Several equally likely

Extended Putative AβS in apoB 32-41

	Residue#		1	2	3	4	5	6	7	8	9	10	11	12				
1	1456-1466			E	V	K	I	D	G	Q	F	R	V	S				B32
2	1468-1478		F	Y	A	K	G	T	Y	G	L	S	C					
3	1486-1496			R	L	N	G	E	S	N	L	R	F	N				
4	1514-1524	D	G	T	L	S	L	T	S	T	S	D	L	Q				
5	1540-1550	N	Y	E	L	T	L	K	S	D	T	N	G	K	Y	K		
6	1554-1564		F	A	T	S	N	K	M	D	M	T	F					
7	1568-1578	N	A	L	L	R	S	E	Y	Q	A	D	Y	E				
8	1596-1606			G	L	E	L	N	A	D	I	L	G	T				
9	1611-1621			S	G	A	H	K	A	T	L	R	I	G				
10	1628-1638	S	T	S	A	T	T	N	L	K	C	S	L	L	V			
11	1640-1650		L	E	N	E	L	N	A	E	L	G	L					
12	1654-1664		A	S	M	K	L	T	T	N	G	R	F	R				
13	1667-1677			N	A	K	F	S	L	D	G	K	A	A	L			B37
14	1679-1689		T	E	L	S	L	G	S	A	Y	Q	A					
15	1692-1702		L	G	V	D	S	K	N	I	F	N	F	K	V			
16	1715-1725			M	M	G	S	Y	A	E	M	K	F	D				
17	1734-1744		A	G	L	S	L	D	F	S	S	K	L	D				
18	1752-1762			F	Y	K	Q	T	V	N	L	Q	L	Q				
19	1765-1775		Y	S	L	V	T	T	L	N	S	D	L	K	Y	N	A	
20	1779-1789		L	D	L	T	N	N	G	K	L	R	L	E				
21	1791-1801			P	L	K	L	H	V	A	G	N	L	K				
22	1820-1830		L	S	A	S	Y	K	A	D	T	V	A	K	V			
23	1835-1845		V	E	F	S	H	R	L	N	T	D	I					
24	1871-1881			S	V	M	A	P	F	T	M	T	I	D	A			B41

$\Delta G_{W\rightarrow O}$ and average $\Delta G_{W\rightarrow O}$ of different a.a. at each of the 12 most common positions of the sequence between B32 and B41

a.a.	1	2	3	4	5	6	7	8	9	10	11	12
$\Delta G_{W\rightarrow O}$	-34.0	45.9	-52.4	79.7	-19.6	103.6	-40.6	100.7	-51.8	137.3	-63.9	106.1
n of a.a.	15	24	24	24	24	24	24	24	24	24	24	19
ave. $\Delta G_{W\rightarrow O}$	-2.67	1.91	-2.18	3.32	-0.82	4.32	-1.69	4.20	-2.16	5.72	-2.66	5.58

***the average $\Delta G_{W\rightarrow O}$ of hydrophobic a.a. at each position is -2.03; while that of hydrophilic a.a. is 4.18.**

Fig. 1. Extended putative amphipathic β strands (AβSs) in the sequence of apolipoprotein B (apoB-32 to apoB-41). Above, the sequence of 24 strands of 11–15 amino acids located between apoB-32 and apoB-41. Below, change in free energy on transferring each residue from water to oil ($\Delta G_{W\rightarrow O}$) and average $\Delta G_{W\rightarrow O}$ of different amino acids (a.a.) at each of the 12 most common positions of the sequence. A 12 amino acid consensus sequence (LSLSLNADLRLK) was derived (see text).

12 amino acid strands were found, including LSL(S/K)l(N/K)A(D/N)LRLK. One of the most likely peptides, LSLSLNADLRLK, called P12, was chosen as the consensus AβS for study. P12 is also one of the six possible consensus sequences derived from the first β region of apoB (apoB-21 to apoB-41). To create a possible amphipathic β sheet, two P12 peptides were linked together in sequence by a short consensus β turn, *NGN*. This peptide, acetyl-LSLSLNADLRLK*NGN*LSLSNADLRLK-amide, is called P27.

EXPERIMENTAL PROCEDURES

Materials

The two peptides, P12 (acetyl-LSLSLNADLRLK-amide) and P27 (acetyl-LSLSLNADLRLK*NGN*LSLSLNADLRLK-amide), which contain two consensus sequences (-LSLSLNADLRLK-) of AβS of apoB linked by the β turn *NGN*, were synthesized by Dr. Robert Carraway at the Peptide Core Facility, University of Massachusetts Medical School (Worcester, MA). Both of the peptides are >95% pure. Dodecane was purchased from EM Science (Gibbstown, NJ). Triolein was from Nu Check Prep (Elysian, MN). 1,1,1,3,3,3-Hexafluoro-2-propanol (99.8+%) (HFIP) was from Aldrich Chemical Co., Inc. (Milwaukee, WI). Ultra-filtered pure water was obtained from Hydro Picosystem (Research Triangle Park, NC) and was used throughout this study. All other reagents were of analytical grade. Stock solutions of both peptides were prepared in HFIP. To do interfacial tension measurements, varied amounts of peptide stocks were added into the aqueous phase surrounding a suspended oil drop (dodecane or triolein) to gain varied peptide concentrations. The maximum ratio of HFIP to water was 1:600. HFIP at this concentration has no effect on the interfacial tension of dodecane or triolein. P12 was studied over a concentration range of 2.9×10^{-7} to 1.5×10^{-5} M, and P27 was studied from 2.2×10^{-7} to 9×10^{-6} M. Both peptides were soluble in the aqueous solution at levels several times greater than the maximum concentrations used in the interfacial studies. Circular dichroic spectra of both peptides show a major peak at 215 nm, consistent with β sheet/strand secondary conformation. The nor-

malized spectra were not significantly changed by wide changes in concentration (P12, 6.6–27 μg/ml; P27, 3.7–59 μg/ml).

Interfacial tension measurement

The interfacial tension of dodecane/water (DD/W) and triolein/water (TO/W) interfaces in the presence of different amounts of P12 or P27 was measured with an I. T. Concept (Longessaigne, France) Tracker oil-drop tensiometer (30) using methods described previously (31). Triolein or dodecane drops (~8 or 10 μl) were formed in gently stirred pure water (6.0 ml) containing a given amount of peptide. Similar studies using a 4 μl air bubble were also carried out. The interfacial tension was then recorded continuously until it approached an equilibrium value. All experiments were carried out at 25 ± 0.1°C in a thermostated system.

Estimation of the surface area per molecule of peptide

From the interfacial tension measurement, the equilibrium interfacial tension (γ) was obtained for each concentration (c) of peptide in the aqueous phase. A plot of γ versus the natural log (ln) c was fitted to a straight line, and the slope of the fitted line $d\gamma/d\ln c$ was obtained. According to the Gibbs equation for the surface (32), the surface concentration (Γ) of an adsorbed molecule, Γ (mol/cm^2) $= -(1/RT)(d\gamma/d\ln c)_{I.P.}$, was estimated. The surface area per molecule of peptide, S(Å^2/molecule) $= 1/(\Gamma \times N)$, where N = Avogadro's number, was obtained for different interfaces.

Compression and expansion of the interfaces

Once the interfacial tension curve approached equilibrium, the oil drop was compressed by rapidly decreasing the volume by ~12% or 25%. The sudden decrease in volume instantaneously decreases the drop surface area and results in a sudden compression, causing the tension (γ) to decrease abruptly. This system was held at this reduced volume for 3–10 min and γ was recorded continuously. If molecules readily desorb from the surface, γ increases back toward the equilibrium value. This is called the desorption curve. If γ does not change, then no net desorption or adsorption occurs. We attempted to estimate the maximum pressure (Π_{MAX}) that the peptide could withstand without being ejected from the surface by plotting the Π immediately after compression against the change in pressure occurring in the next 3–10 min as described previously (31). However, on both DD/W and TO/W interfaces there was no change, indicating that the peptide concentration at the surface remained unchanged and no peptide was desorbed in the 3–10 min time frame. Only at the air/water (A/W) interface could a Π_{MAX} be estimated for P27 (see Results). To expand the surface, the volume of the oil droplet was rapidly increased by ~25% or 12%, which suddenly increases the area and as a result γ abruptly increases. If molecules adsorb from the bulk phase to adhere to the newly formed extra surface, then γ will decrease back toward equilibrium. This is called the adsorption curve.

Elasticity of the surface at the equilibrium surface tension

After the tension curve has reached an equilibrium value, oscillations of the volume can be made at different amplitudes and periods (i.e., frequencies). The standard protocol for oscillations was carried out using an 8 or 10 μl droplet of dodecane or triolein in water with various added amounts of P12 or P27. The γ was allowed to reach near equilibrium values (**Fig. 2**), and then the drops were oscillated at different periods ranging from 8 to 128 s (0.125–0.008 Hz) at amplitudes of approximately ±10%, ±20%, or ±25%. As the volume (V) was oscillated in a sinusoidal manner, the interfacial area (A) and surface tension (γ) were recorded continuously, and the phase angle (ϕ) between compression and expansion was computed. The interfacial elasticity modulus (ε) was derived ($\varepsilon = d\gamma/d\ln A$). The elasticity real part (ε') and the elasticity imaginary part (ε'') were obtained ($\varepsilon' = |\varepsilon| \cos\phi$, $\varepsilon'' = |\varepsilon| \sin\phi$) (33, 34).

Elasticity as a function of surface pressure

To calculate the elasticity modulus as a function of surface pressure generated by the peptide monolayer at the surface, continuous oscillations were carried out 10 s after an oil drop was formed in the peptide solution. Allowing 10 s to form the drop permitted the system to stabilize, and then the volume was oscillated by approximately ±12% or ±25% at different periods continuously until the mean interfacial tension approached equilibrium. This gave a continuous measurement of the mean surface tension (and surface pressure), ε, ε', ε'', and ϕ. The surface tension of the interface without peptide (γ_0) minus the surface tension of the interface with peptide ($\gamma_{peptide}$) is the surface pressure (Π), i.e., $\Pi = \gamma_0 - \gamma_{peptide}$.

RESULTS

The adsorption of P12 and P27 to DD/W and TO/W interfaces

Figure 2 shows typical sets of curves illustrating the effect of concentration on the adsorption isotherms of P12 and P27 at the DD/W interface (A, B) and the TO/W interface (C, D). When no peptide is on the surface, the interfacial tension is ~52 mN/m at the DD/W interface and ~32 mN/m at the TO/W interface. Peptide P12 on DD/W (Fig. 2A) decreases the interfacial tension at its highest concentration (curve e) to ~20 mN/m in 1,500 s. In the most dilute concentration (curve a), there is considerable noise at the beginning of the experiment (first 100 s) and only a small change in the interfacial tension for some 300 s. This initial slow-change interfacial tension is called the "lag phase" and is probably related to the peptide adsorbing to the interface but at inadequate concentrations to change surface tension significantly. As the bulk concentration increases (curve b), the lag period shortens, and it virtually disappears at higher concentrations (curves d, e). The region of the curve where there is the most rapid change in interfacial tension with time ($d\gamma/dt$) is related to the peptide saturating the surface and producing peptide/peptide contact. This most rapid change in the curve ($d\gamma/dt$) is estimated from a line drawn through the most rapidly descending part of each curve and is directly dependent on the concentration (Fig. 2A, inset). This probably indicates that the rate of peptide saturation of the surface is proportional to the peptide concentration. As the surface saturates, the surface tension begins to decrease much more slowly and moves toward an equilibrium value. Because the surface pressure (Π) produced is equal to the surface tension of the interface without peptide (γ = 52 mN/m) minus the final surface tension near equilibrium ($\gamma_{peptide}$ = 20 mN/m), then P12 develops at least 32 mN/m pressure at the highest concentration studied by 1,500 s. On the DD/W interface, the longer peptide P27 shows similar behavior, but at a lower concentration. The maximum decrease of the interfacial tension for P27 occurs at 6.6 × 10^{-6} M

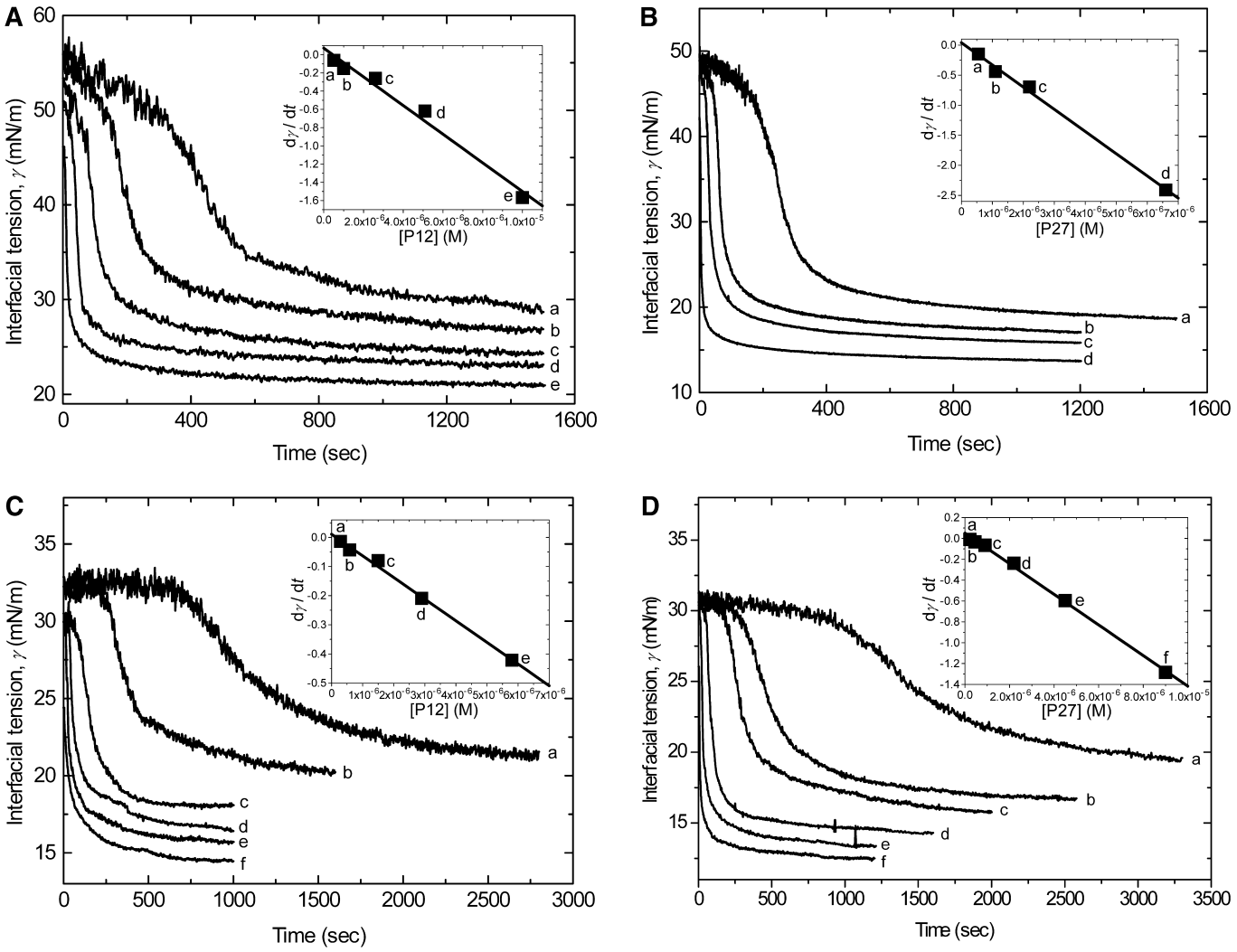

Fig. 2. Interfacial tension (γ) versus time curves of P12 and P27 at dodecane/water (DD/W) or triolein/water (TO/W) interfaces. An 8 μl dodecane or triolein drop was formed in pure water with varied amounts of P12 or P27, respectively. All experiments were carried out at 25 ± 0.1°C. Insets show the slopes ($d\gamma/dt$) of the steep part of the tension curves plotted against the molar concentration of peptides, and linear regression was made to the plots. A: P12 at the DD/W interface. a, 5.1×10^{-7} M; b, 1.0×10^{-6} M; c, 2.6×10^{-6} M; d, 5.1×10^{-6} M; e, 1.0×10^{-5} M. For the regression line in the inset, $R = -0.99$, $P = 0.00118$; the slope is -1.6×10^5. B: P27 at the DD/W interface. a, 5.5×10^{-7} M; b, 1.1×10^{-6} M; c, 2.2×10^{-6} M; d, 6.6×10^{-6} M. For the regression line in the inset, $R = -0.998$, $P = 0.00185$; the slope is -3.7×10^5. C: P12 at the TO/W interface. a, 2.9×10^{-7} M; b, 5.8×10^{-7} M; c, 1.5×10^{-6} M; d, 2.9×10^{-6} M; e, 5.8×10^{-6} M; f, 1.5×10^{-5} M. For the regression line in the inset, $R = -0.997$, $P = 0.00016$; the slope is -7.4×10^4. The inset does not include point f because the slope cannot be measured. D: P27 at the TO/W interface. a, 2.2×10^{-7} M; b, 4.5×10^{-7} M; c, 9.0×10^{-7} M; d, 2.2×10^{-6} M; e, 4.5×10^{-6} M; f, 9.0×10^{-6} M. For the regression line in the inset, $R = -0.99$, $P = 0.00118$; the slope is -1.6×10^5.

rather than at 1×10^{-5} M for P12. Furthermore, the surface tension at the highest concentration of P27 decreases to ~13 mN/m, somewhat lower than that for P12. This corresponds to P27 producing a surface pressure (Π) of at least 39 mN/m.

Figure 2C, D show the adsorption isotherms of P12 and P27, respectively, at the TO/W interface. Both peptides show an appreciable lag phase at the lowest concentration, which decreases as the concentration increases. Also, the slope of the steep part of the curve ($d\gamma//dt$) is concentration dependent (inset), similar to the peptides on the DD/W interface. The interfacial tension tends toward equilibrium more quickly at high concentrations than at low concentrations. After 1,000 s, the longer peptide P27 decreases the interfacial tension to ~12 mN/m, whereas P12 decreases it to ~14 mN/m. Thus, both peptides decrease the interfacial tension of triolein in a concentration- and time-dependent manner. Both peptides also decrease γ in a time-dependent manner at the A/W interface (data not shown). On the A/W interface, P12 was studied at concentrations between 2.4×10^{-7} M and 1.2×10^{-5} M. At the highest concentration, P12 decreases γ to ~37 mN/m. P27 decreases γ to ~38 mN/m at 8.9×10^{-6} M.

Estimation of the surface area at saturation of P12 and P27 using the Gibbs adsorption isotherm equation

The Gibbs equation can be used to estimate the area of small molecules adsorbed to a surface. However, it is not

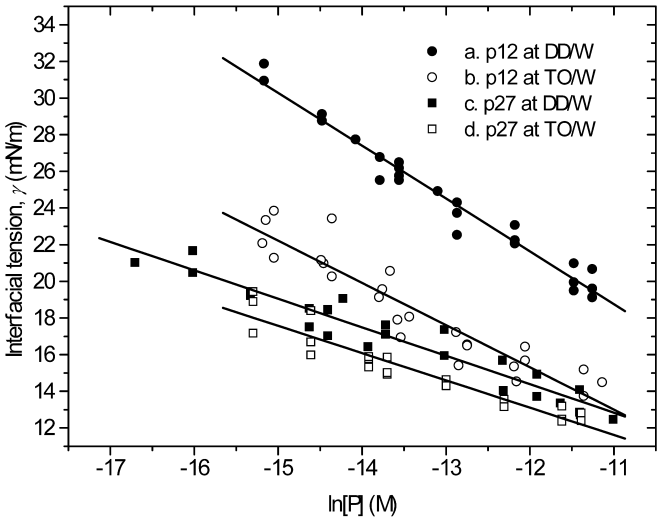

Fig. 3. Equilibrium interfacial tension (γ) of DD/W and TO/W interfaces with P12 or P27 plotted against the natural log (ln) molar concentration of peptides in the aqueous phase. Each point is a separate measurement. Several measurements were carried out at each peptide concentration. The equations for the lines, the estimate surface concentration Γ, and area per molecule peptide are listed in Table 1.

generally valid for use with proteins because of several problems, including conformational changes or denaturation at the interface, irreversible adsorption, or the formation of multilayer. Because these peptides are relatively small and have well-defined hydrophobic and hydrophilic surfaces (Fig. 1) and are in the β conformation in solution, we reasoned that they would adsorb to the interface in the β conformation with the hydrophobic side in the oil and the hydrophilic side in the water. We therefore used the Gibbs equation to attempt to estimate the concentration of the peptide at the interface. The values obtained appear to validate the use of the Gibbs equation for these small peptides. The equilibrium values (γ) for each peptide concentration were plotted against the natural log (ln) of the aqueous peptide concentration in **Fig. 3**. The slope $d\gamma/d \ln c$ was used to calculate the excess surface concentration (Γ) at the interface using the equation $\Gamma = -(1/RT)(d\gamma/d \ln c)$. The estimated surface concentration and area per molecule (Å^2) are given in **Table 1**. These values suggest that each amino acid at the interface occupies between 11.2 and 15.1 Å^2. This is consistent with an AβS lying with all of the hydrophobic amino acids in the oil interface, with each hydrophobic residue covering ~22–30 Å^2 of interface. A predicted area for an amino acid from the anti-parallel β strand lattice suggests an area of ~15 Å^2 per amino acid. The area per residue of an α helical consensus sequence peptide (CSP) is similar when studied under nearly identical conditions at the DD/W interface (Table 1) (31).

Compression and expansion of the interface

Figure 4 shows examples of compression and expansion of the surface at approximately equilibrium surface tension. Figure 4A shows P27 at 2.33×10^{-6} M at the DD/W interface. After 3,730 s, the interfacial tension had decreased to near equilibrium at ~12.5 mN/m. The volume was then suddenly decreased from 8 to 6 μl, giving rise to a sudden decrease in the area and a decrease in the interfacial tension to ~9 mN/m. The system is allowed to remain at this volume and area and the surface tension is followed for several minutes. The surface tension does not change, indicating that the peptide is not being desorbed from the surface, even though the pressure has increased by more than 4 mN/m. After several minutes with no change in the surface tension, the volume is increased to ~10 μl, causing an immediate increase in the area and a corresponding rapid increase in the interfacial tension. Because new surface is created by the expansion, new molecules from the aqueous solution adsorb to the surface and the interfacial tension rapidly decreases and gradually moves toward an equilibrium value. An example of P12 spread at a triolein drop is shown in Fig. 4B using a similar protocol. After 2,270 s, the interfacial tension approaches an equilibrium value of ~12 mN/m, and then the volume suddenly decreases from ~10 to ~8 μl, a decrease of 20%. The area correspondingly decreases and the interfacial tension decreases abruptly to ~4 mN/m. Virtually no change occurs in the interfacial tension over the next few minutes, indicating that even at this low surface tension (or high surface pressure) P12 is not being expelled from the surface. The volume is then increased to ~12 μl, causing an abrupt increase in the area and interfacial tension. This increase in area produces new sur-

TABLE 1. Estimated surface concentration (Γ) and surface area per molecule of amphipathic β strand peptides (area)

Interfaces	Equation of the Fit Line	R^2	Γ	Area	Area/Amino Acid
			mol/cm^2		*Å*^{2}
P27 DD/W	Y = −1.5535X − 4.256	0.9264	6.2×10^{-11}	268	11.2
P27 TO/W	Y = −1.4883X − 4.752	0.9076	5.9×10^{-11}	280	11.7
P12 DD/W	Y = −2.8816X − 12.943	0.9674	1.2×10^{-10}	144	12
P12 TO/W	Y = −2.3029X − 12.326	0.8744	9.2×10^{-11}	181	15.1
CSP DD/W[a]	Y = −0.6696X − 12.904	0.8312	2.7×10^{-11}	622	14

DD/W, dodecane/water; TO/W, triolein/water.

[a] Data are from ref. (31). CSP, an amphipathic α-helix consensus peptide derived from the water-soluble human apolipoproteins apoA-I, apoA-IV, and apoE with the sequence (PLAEELRARLRAQLEELRERLG)2-NH_2.

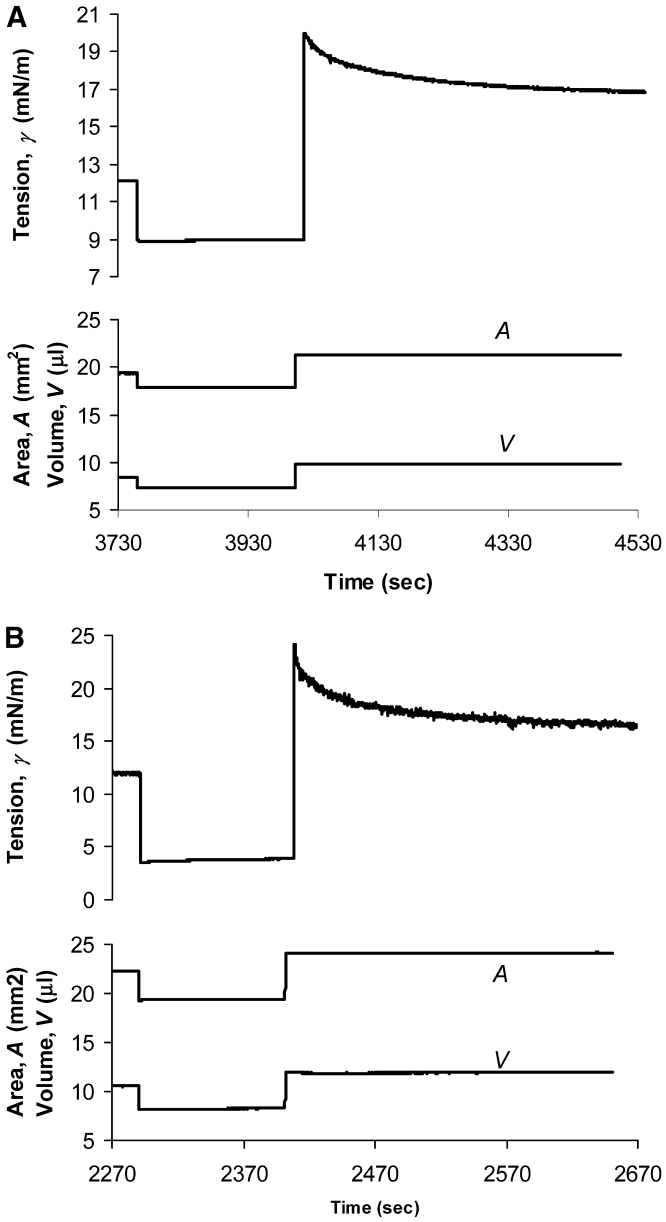

Fig. 4. Examples of changes in interfacial tension (γ) under compression and expansion of the interfaces. A: An 8 μl dodecane drop in an aqueous phase containing 2.3×10^{-6} M P27 was compressed and expanded by ~25% (±2 μl). B: A 10 μl triolein drop in an aqueous phase containing 4.8×10^{-6} M P12 was compressed and expanded by ~20% (±2 μl). In both cases, after compression, γ decreased immediately but did not change during the ~5 min period while the decreased volume was kept constant. After expansion of the interfaces, γ increased accordingly and moved back to equilibrium values, because peptides in the aqueous phase adsorbed onto the new interfacial space generated by expanding the interface. All experiments were carried out at 25 ± 0.1°C in pure water.

face to which P12 can adsorb, decreasing γ rapidly at first and then more slowly toward an equilibrium.

In other compression and expansion experiments, both peptides were studied at both DD/W and TO/W interfaces under different conditions. We found that increasing the pressure by up to 8 mN/m above equilibrium pressure failed to detach the peptide from the interface

TABLE 2. Maximum pressure Π_{MAX} of different peptides at varied interfaces

Interfaces	CSP	P27	P12
A/W	21.3[a]	~33	N/A
DD/W	31.7[a]	>43	>42
TO/W	16[b]	>25	>27

Values shown are mN/m. A/W, air/water; N/A, not applicable.
[a] Data are from ref. (31).
[b] Unpublished data.

over a period of several minutes. Further compression often causes the drop to detach. From compressions on the DD/W interface up to 44–45 mN/m (γ = 8–7 mN/m), we estimate the Π_{MAX} to be >42 mN/m for P12 and >43 mN/m for P27. At the TO/W interface, Π_{MAX} was estimated to be at least 27 and 25 mN/m for P12 and P27, respectively (**Table 2**). For comparison, compression and expansion experiments of P27 at the A/W interface were carried out as well. P27 at the A/W interface appeared to desorb above a pressure of 33 mN/m (data not shown). These values are compared with a CSP derived from exchangeable apolipoproteins apoA-I, apoA-II, and apoE (31) in Table 2. The Π_{MAX} for CSP is at least 10 mN/m lower than P12 and P27 on all surfaces. These studies indicate that the compression of P12 and P27 by up to 25% on the DD/W or TO/W interface is not adequate to desorb those peptides from the interface. This means that if the starting area of both peptides at equilibrium was ~15 Å² per amino acid, it could be compressed to almost 11 Å² per amino acid without detaching the peptide from the interface. However, when the interface is expanded above the equilibrium value, then new peptide can adsorb to the new space formed at the interface and decrease the surface tension back toward an equilibrium value.

Elastic behavior of the peptides at equilibrium surface tension

After the peptide was spread at the interface, it was allowed to approach equilibrium, as indicated in Fig. 2, and then the drop volume was oscillated in a standard protocol (31) varying the oscillation period between 8 and 12 s. In special cases, oscillations were carried out for longer periods, up to 128 s. The volume was oscillated at ±12.5%, ±20%, or ±25% and the data were analyzed for changes in volume (V), area (A), and interfacial tension (γ). A typical experiment for P27 (2.33×10^{-6} M) on the DD/W interface is shown in **Fig. 5A**; an 8 μl dodecane drop was oscillated ±2 μl at a period of 10 s. In Fig. 5B, a 10 μl triolein drop with P12 was oscillated ±2 μl at a period of 12 s. In both examples, the V, A, and γ changed virtually in phase. From the simultaneous change in A and γ, the following parameters were calculated: the surface viscoelastic modulus ($\varepsilon = d\gamma/d \ln A$), the phase angle (ϕ) in degrees between compression and expansion, the elastic or "real" component of the modulus (ε'), and the imaginary viscous component of the modulus (ε''). The imaginary component is reflected in the phase difference between the stress ($d\gamma$) and the strain ($d \ln A$). If the phase angle

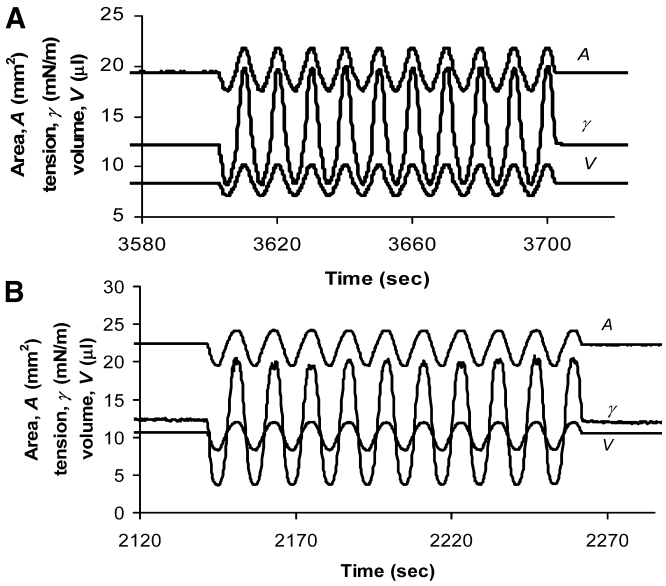

Fig. 5. Examples of oscillations around equilibrium interfacial tension of P12 and P27 at the DD/W or TO/W interface. A: An 8 μl dodecane drop in an aqueous phase containing 2.3×10^{-6} M P27 was oscillated at 8 ± 2 μl at 10 s. B: A 10 μl triolein drop in an aqueous phase containing 4.8×10^{-6} M P12 was oscillated at 10 ± 2 μl at 12 s.

approaches zero, then the surfaces can be considered completely elastic and the elastic modulus ε is equal to ε'. The calculated elasticity parameters of several experiments are presented in **Table 3**. For P27 on the DD/W interface, the mean surface tension γ (the tension averaged over the oscillation period) decreases from ~16 to 1 mN/m as the concentrations decrease; these values are close to the equilibrium interfacial tension for given concentrations. The phase angle ϕ in some of these experiments is either negative, which is an artifact of the system, or very minor (not significantly different from zero), indicating that P27 on the DD/W interface is purely elastic. P27 on the TO/W interface, P12 on the DD/W interface, and P12 on the TO/W interface are also almost purely elastic, because the ϕ is always less than 8°. Thus, most of the energy that is put in to compress the surface is regained when the surface is expanded. The elastic modulus ε is ~50 mN/m for P27 and somewhat higher for P12. Similar experiments with P27 at the A/W interface also show nearly purely elastic behavior, because the phase angle ϕ is 8° or less (Table 3).

Elastic behavior as a function of surface pressure

Continuous oscillation starting a few seconds after forming a drop allows a continuous plot of γ, V, and A with time, from which the phase angle, ϕ, and the elastic modulus, ε, can be calculated as a function of time. After forming an oil drop in a peptide solution, the drop is allowed to stabilize for 10 s and then a continuous oscillation is begun as the surface tension gradually decreases toward an equilibrium value. This allows a plot of the modulus, ε, versus the surface pressure ($\Pi = \gamma - \gamma_{peptide}$). Examples of P27 at the DD/W interface are shown in **Fig. 6**. At very low Π (<12 mN/m), the modulus increase in a linear manner with the slope is ~2 ε/Π. This is consistent with an ideal surface of dispersed peptide with little or no peptide-peptide interaction. At Π from ~15 mN/m up to ~22 mN/m, the slope of the line gave a greater increase in ε/Π ratio, indicating molecule-molecule interaction at the interface. Above 25 mN/m, the modulus plateaus and then decreases slightly at very high pressures, indicating a maximum ε beyond this Π. Finally, over a wide range of pressure, the surface retains its elasticity, because ϕ does

TABLE 3. Dynamic interfacial properties of P27 and P12 at different interfaces

Interfaces	Peptide Concentration	$\Delta V / V$	Period	Mean γ	ε	ϕ	ε'
	M	± %	*s*	*mN/m*	*mN/m*	°	*mN/m*
P27 at DD/W	5.4×10^{-7}	25	128	16.2	76.0	0.7	76.0
	2.3×10^{-6}	25	10	13.1	53.2	−6.1	52.9
	4.3×10^{-6}	25	8	12.6	45.4	−2.3	45.3
	4.3×10^{-6}	25	32	11.8	32.6	0.7	32.6
	4.7×10^{-6a}	25	12	12.2 ± 0.1	45.1 ± 3.6	−1.4	45.0 ± 3.6
P27 at TO/W	4.7×10^{-6b}	20~25	12	11.6 ± 0.4	51.8 ± 4.6	−0.5	51.7 ± 4.7
P12 at DD/W	4.8×10^{-6c}	12.5	8	13.0	113.3	−11	111.3
P12 at TO/W	4.8×10^{-6d}	20~25	12	11.7	82.0	−5.3	81.6
P27 at A/W	1.1×10^{-6}	25	8	43	139.5	3.4	139.2
	1.1×10^{-6}	25	32	41.4	131.4	3.9	131.1
	1.1×10^{-6}	25	128	39.4	122.3	4.2	122.0
	4.3×10^{-6}	25	8	37.1	106.6	4.4	106.2
	4.3×10^{-6}	25	32	35.7	94.8	6.6	94.1
	4.3×10^{-6}	25	128	34.4	87.9	8.2	87.0

All oscillation experiments were carried out in pure water or pH 7.4 phosphate buffer (2 mM) at 25 ± 0.1°C. V, initial drop volume; ΔV, oscillation amplitude; mean γ, mean interfacial tension of equilibrium oscillation; ε, viscoelastic modulus; ϕ, viscous phase angle, a phase difference between $d\gamma$ and dA; ε', elastic component, the real part of ε.

[a] Average of three measurements with the same V and ΔV and very similar periods (12 and 14 s).

[b] Average of three measurements with the same ΔV and period and very close V (10 and 8 μl).

[c] Average of two measurements with the same V, ΔV, and period.

[d] Average of two measurements with the same ΔV and period and very close V (10 and 8 μl).

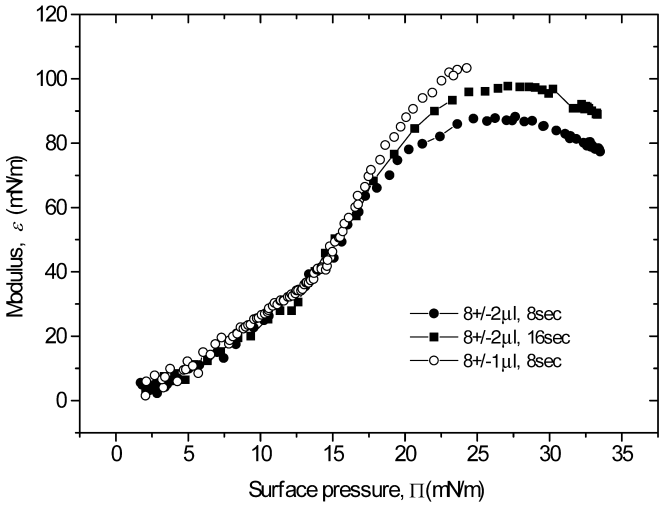

Fig. 6. Elasticity modulus (ε) plotted against the mean surface pressure (Π) of P27 at the DD/W interface. The concentration of P27 in the aqueous phase was 5.4×10^{-7} M.

not exceed 10° (data not shown). Similar data were obtained at the A/W interface for P27 (data not shown).

DISCUSSION

ApoB has been divided into five super domains of putative secondary structure (3, 13, 14). The first domain is made up of α and β structures comprising the first 20.5% of apoB and is a necessary component for the secretion of apoB (3, 15–17). It has high homology to lipovitellin (18–20) but binds very little lipid and is secreted in essentially lipid-free form. The second domain is made up largely of putative amphipathic β sheets (22), and it is within this domain that lipid is recruited and a nascent lipoprotein with a TAG core is assembled (4–8, 12). Analysis of the sequence between apoB-21 and apoB-41 detects 41 AβSs of 11–15 amino acids in length (22). We have aligned these strands and computed a consensus sequence of AβS of 12 amino acids (P12) as being one of several possible consensus sequences for this entire region. It is also a consensus sequence for the region between apoB-32 and apoB-41 (Fig. 1), which seems to recruit TAG when there is very low expression of MTP (7); that is, the secondary structure seems to be the main driving force for TAG recruitment.

A consensus peptide common to strands in apoB-32 to apoB-41 and in apoB-21 to apoB-41, P12 (LSLSLNADLRLK), was synthesized and purified. Furthermore, a dimer of P12 linked together with a β turn, *NGN*, to produce a putative amphipathic two β-stranded sheet was synthesized, and these two peptides were studied at DD/W, TO/W, and A/W interfaces using an interfacial tensiometer (30), which allows interfacial tension to be analyzed with time and the surface to be compressed or expanded by changing the volume and to be oscillated to examine the elastic properties of the peptides adsorbed at the interface (31). Both peptides appear to occupy ~11–15 Å^2 per amino acid at saturation. We have shown that both P12 (AβS) and P27 (putative amphipathic sheet) adsorb to these interfaces in a time- and concentration-dependent manner. They decrease the interfacial tension to a marked degree and form a stable interface. These peptides are extremely difficult to displace from the dodecane and triolein interfaces, even at high surface pressure. This may indicate extensive H-bonding between strands. This behavior contrasts to the 44 amino acid amphipathic α helix peptide modeled after a consensus sequence of type A α helices derived from apoA-I, apoA-II, and apoE called CSP, which we reported earlier (31). CSP also decreases γ of the A/W and oil/water interfaces (31), but under identical conditions its effect is less. For instance, at the DD/W interface and a concentration of $1.1–1.2 \times 10^{-6}$ M, CSP produces a pressure of 29 mN/m at 20 min, whereas P27 produces a pressure of 35 mN/m. Furthermore, CSP is displaced above a certain pressure called Π_{MAX} into the aqueous medium, whereas P12 and P27 are not (Table 2). The β strand (P12) and β sheet (P27) peptides show nearly pure elastic behavior at the interface and can be compressed by up to 25% while still retaining their elasticity without desorbing from the interface. On the other hand, the amphipathic α helical peptide (CSP) only shows elastic behavior when compressed rapidly to a limited degree (~6%). When CSP is compressed to a greater extent (i.e., 25%), it is forced off the interface into the aqueous phase, which leads to its viscoelastic behavior at the interface (31).

The adsorption of P12 and P27 to the hydrocarbon surface (dodecane) is a thermodynamically highly favorable process. If we assume that the area of each amino acid at the interface at saturation is ~12 Å^2 (Table 1), because every other residue points 180° in the opposite direction, then each amino acid on the hydrophobic side covers 24 Å^2 of hydrocarbon surface. The change in interfacial free energy when peptide adsorbs to the interface is derived from the difference in γ of the pure hydrocarbon/water interface (52 mN/m) and with peptide adsorbed. Because P12 reduces γ to ~14 mN/m, $\Delta\gamma = -38$ mN/m. Therefore, each mole of hydrophobic amino acid occupying 24 Å^2 per molecule reduces the $\Delta G_{W\rightarrow O}$ surface by 1.31 kcal, that is, $\Delta\Delta G_{W\rightarrow O} = -1.31$ kcal/mol hydrophobic residue.

Therefore, by covering the hydrocarbon surface with peptide, the free energy of that surface is reduced. Furthermore, P12 and P27 are soluble and probably monomeric in the low concentrations used in this study. In solution, the hydrophobic amino acids are exposed to water. When they bind to dodecane, they are transferred to the hydrocarbon surface, again a favorable process. The mean change in free energy on transferring the five leucines and one alanine from water to oil, using the standard GES scale (28, 29), is −2.43 kcal/mol hydrophobic amino acid. In sum, the binding of peptides to hydrocarbon is energetically highly favorable, yielding a reduction of $-1.31 + -2.43 = -3.74$ kcal/mol hydrophobic amino acid if each hydrophobic amino acid covers 24 Å^2 per molecule.

A number of studies on synthetic model AβS peptides with alternating hydrophobic and charged residues have been carried out at the A/W or 0.1 M KCl interface, and the peptides were shown to lie flat on the surface (35, 36).

The synthetic peptide poly(leu-lys)$_n$, abbreviated here $(LK)_n$, where n was 8 or 10, was studied at 0.1 M KCl at pH ~5.6 by Régine, Lelièvre, and Brack (35). The spreading pressure Π_S measured by placing a small amount of the dry peptide powder on the 0.1 M KCl interface produced ~21–26 mN/m pressure. However, when spread from a 9:1 HFIP/water solution on the 0.1 M KCl interface on a Langmuir trough, the peptides could be compressed to 47 mN/m without collapsing, indicating a large region of metastable interface between 26 and 47 mN/m. The minimal area at liftoff (i.e., extrapolated to 0 pressure) for $(LK)_{10}$ was ~21 Å^2 per residue, and that at the collapse was ~15 Å^2 per residue, indicating that they were lying flat on the surface up to collapse. The peptide showed low compressibility but could be compressed by ~25% before collapse. The slightly large area at liftoff may reflect the fact that the lysines are ionized at pH 5.6; therefore, charge repulsion might expand the area. When $(LK)_8$ was placed in the aqueous phase, the interfacial Π gradually increased with time, as it absorbed to the surface to a value similar to the spreading pressure. The highest concentration of $(LK)_8$ used in the absorption studies (1.4×10^{-5} M) produced a surface pressure of ~30 mN/m. This compares to P12, which produces a Π of 35 mN/m at a similar concentration. Castano, Desbat, and Dufourcq (36) studied idealized amphipathic β sheet peptides $(LK)_nK$ (n = 4–7) labeled at the N terminus with a fluorescent dansyl probe. All peptides were monomeric at 2 μM. Peptides were spread on a Langmuir balance on 0.13 M NaCl buffered to pH 7.5 at 20–25°C. Using the polarization-modulated-infrared-reflection-absorption spectroscopy technique, they deduced that at a pressure of ~20 mN/m the peptides lay flat on the surface and form anti-parallel β sheets. They state that "the flat orientation is also lateral pressure independent."

Rapaport et al. (37) used grazing incidence X-ray diffraction (GIXD) to study the two-dimensional structure of model amphipathic β sheet peptides at the A/W interface. They first studied the β sheet-forming peptide [(ala-gly)$_3$ glu-gly]$_{36}$ at the interface and after compression used GIXD to record diffractions. This peptide showed a very weak 4.7 Å spacing at the interface, indicating some β sheet formation at the interface. The 4.7 Å spacing is the spacing between the hydrogen-bonded β strands. In a clever design of a peptide to prevent random hydrogen bond formation between different strands, they blocked the ends of the peptide with prolines. The peptide pro-glu (phe-glu)$_4$ pro, when compressed on an acid (pH < 5) interface, has a liftoff area of ~15 Å^2 per amino acid and an area of ~12.5 Å^2 per amino acid at monolayer collapse (30 mN/m). GIXD showed a two-dimensional crystal of ~460 × 430 Å^2 on the interface at low pressure. The two-dimensional lattice of this interesting peptide was a = 4.7 Å^2 (distance between H-bonded chain) and b = 37.4 Å (chain length). This indicates that ~90 strands lie parallel and in register from one of the two-dimensional axes and ~12 peptides lie in register end to end. The film thickness was estimated at 8 Å, a reasonable thickness for this AβS lying flat on the surface. The activated total reflectance infrared spectrum of the same system indicated an antiparallel sheet. The area per amino acid in the two-dimensional crystal lattice consisting of 11 amino acids has a surface area parallel to the interface of ~176 Å^2, to give each amino acid ~16 Å^2. The peptide spread between pH 4 and 5.3 was quite stable and gave similar data; however, when the peptide was spread at pH 7 or above, it disappeared from the interface and went into solution. This indicates that the glutamic acid must be nonionized for these two-dimensional β sheets to form. The authors propose hydrogen bonding lattice of the glutamic acids between the individual sheets. Most interestingly, when the surface pressure isotherms were obtained for this peptide at pH 4, the limiting area at liftoff pressure (zero pressure) was ~15 Å^2 per amino acid and could be compressed up to ~30 mN/m, at which point it collapsed. At 30 mN/m, the area is estimated at ~12.5 Å^2 per amino

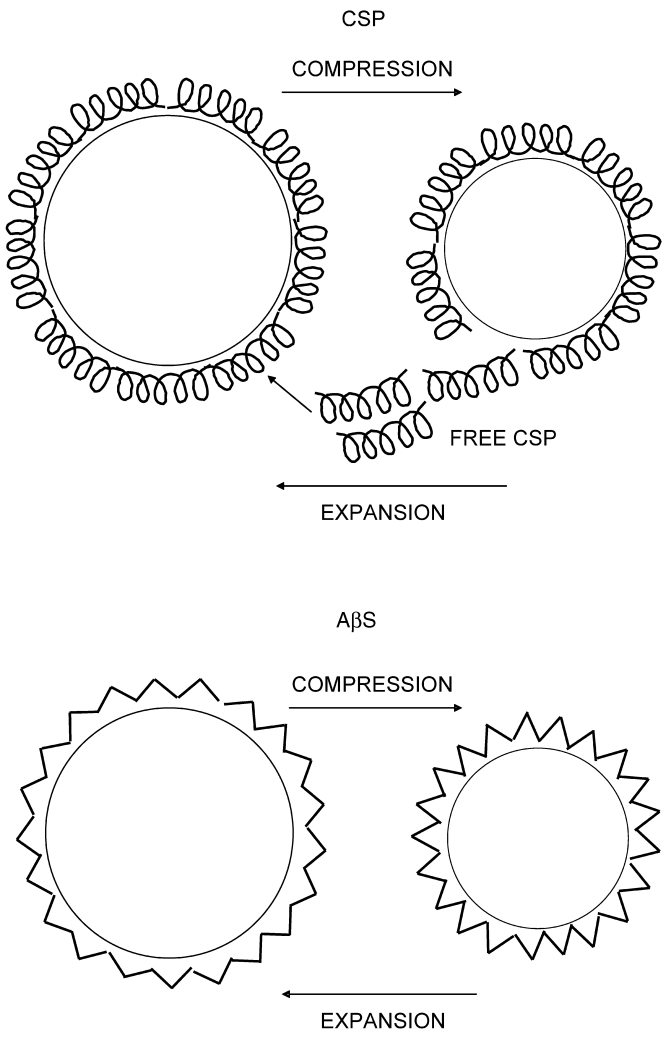

Fig. 7. A schematic model for the surface behavior of amphipathic α helix [consensus sequence peptide (CSP)] and AβSs on hydrophobic interfaces. After the interface reached an equilibrium γ, it was saturated with peptides (left side). When the interface was compressed, CSP was ejected from the interface into the aqueous phase, whereas AβSs (P12 and P27) stayed on the interface without being pushed off. The area of AβSs could be reduced by up to 25% and still retain its elastic behavior.

acid. That this peptide can be compressed ~20% before collapsing is somewhat similar to the decrease in area on compression of P12 and P27 in the present study. Using a similar amphipathic motif, Rapaport et al. (38) placed two proline turns into a 30 amino acid tri-stranded peptide. The liftoff area near zero pressure was ~460 Å or 15.3 Å per amino acid, and estimated unit cell from the GIXD indicated an area of ~500 Å^2 and ~16.7 Å^2 per amino acid. Thus, both appropriately engineered strands and sheets can form two-dimensional crystals at the A/W interface that are characterized by the hydrophilic amino acids being in the aqueous phase and the hydrophobic residues in the air and peptide chain being parallel to the interface.

Our peptide is not an idealized amphipathic strand but rather a consensus peptide derived from the sequences that are responsible for recruiting TAG in the interface. These peptides occupy areas at saturation of ~12–15 Å^2 per amino acid, but they can be compressed by ~25% without being extruded (collapsed) out of the surface. They also exhibit an extraordinarily almost complete elasticity and are able, like a spring, to be compressed and expand elastically. Furthermore, when compressed to high pressures (>42 mN/m), they are not forced off the surface. Thus, these kinds of amphipathic strands and sheets make an excellent anchor for apoB at the interface between the core TAG or in cholesteryl ester VLDL. On the other hand, we have previously shown that the consensus amphipathic α helical peptide CSP (31), of which there are at least two super domains present in apoB (3, 13, 14), are less elastic and can only be compressed a few percentage points before being extruded from the surface. Thus, it is our hypothesis, as shown in **Fig. 7**, that when the pressure is low, both amphipathic α helices and AβSs are at the interface. However, as the pressure increases, for instance during the formation of surface components (fatty acid and monoacylglycerols) during lipoprotein lipase triglyceride hydrolysis, then the surface pressure increases and those peptides, like CSP, with low extrusion pressure Π_{MAX}, are forced off the surface into the aqueous solution. When the surface pressure decreases, they can readsorb to the surface. In contrast, AβSs like P12 and P27 can withstand high pressure and retain their elasticity. If both types of peptides existed in the same apolipoprotein (e.g., apoB), they would allow surface flexibility as surface pressure and composition changed within the lipoprotein.

This work was supported in part by National Heart, Lung, and Blood Institute (National Institutes of Health) Grant 2P01 HL-26335-21. The authors thank Dr. David Atkinson, Dr. Haya Herscovitz, and Dr. Margaretha Carraway for support and suggestions on this work. The authors also thank Donna Ross for manuscript preparation.

REFERENCES

1. Atkinson, D., and D. M. Small. 1986. Recombinant lipoproteins: implications for structure and assembly of native lipoproteins. *Annu. Rev. Biophys. Biophys. Chem.* **15:** 403–456.
2. Zambon, A., S. S. Deeb, P. Pauletto, G. Crepaldi, and J. D. Brunzell. 2003. Hepatic lipase: a marker for cardiovascular disease risk and response to therapy. *Curr. Opin. Lipidol.* **14:** 179–189.
3. Segrest, J. P., M. K. Jones, H. DeLoof, and H. Dashti. 2001. Structure of apolipoprotein B-100 in low density lipoproteins. *J. Lipid Res.* **42:** 1346–1367.
4. Yao, Z. M., B. D. Blackhart, M. F. Linton, S. M. Taylor, S. G. Young, and B. J. McCarthy. 1991. Expression of carboxyl-terminally truncated forms of human apolipoprotein B in rat hepatoma cells. Evidence that the length of apolipoprotein B has a major effect on the buoyant density of the secreted lipoproteins. *J. Biol. Chem.* **226:** 3300–3308.
5. Graham, D. L., T. J. Knott, T. C. Jones, R. J. Pease, C. R. Pullinger, and J. Scott. 1991. Carboxyl-terminal truncation of apolipoprotein B results in gradual loss of the ability to form buoyant lipoproteins in cultured human and rat liver cell lines. *Biochemistry.* **30:** 5616–5621.
6. Boren, J., L. Graham, M. Wettesten, J. Scott, A. White, and S. O. Olofsson. 1992. The assembly and secretion of ApoB 100-containing lipoproteins in Hep G2 cells. ApoB 100 is cotranslationally integrated into lipoproteins. *J. Biol. Chem.* **267:** 9858–9867.
7. Carraway, M., H. Herscovitz, V. Zannis, and D. M. Small. 2000. Specificity of lipid incorporation is determined by sequences in the N-terminal 37 of apoB. *Biochemistry.* **39:** 9737–9745.
8. Herscovitz, H., M. Hadzopoulou-Cladaras, M. T. Walsh, C. Cladaras, V. Zannis, and D. M. Small. 1991. Expression, secretion, and lipid-binding characterization of the N-terminal 17% of apolipoprotein B. *Proc. Natl. Acad. Sci. USA.* **88:** 7313–7317.
9. Herscovitz, H., D. Gantz, A. M. Tercyak, V. Zannis, and D. M. Small. 1992. Expression of human apolipoprotein E but not that of apolipoprotein A-I by mouse C127 cells is associated with increased secretion of lipids in the form of vesicles and discs. *J. Lipid Res.* **33:** 791–803.
10. Herscovitz, H., A. Kritis, I. Talianidis, E. Zanni, V. Zannis, and D. M. Small. 1995. Murine mammary-derived cells secrete the N-terminal 41% of human apolipoprotein B on high density lipoprotein-sized lipoproteins containing a triacylglycerol-rich core. *Proc. Natl. Acad. Sci. USA.* **92:** 659–663.
11. Sellers, J. A., and G. S. Shelness. 2001. Lipoprotein assembly capacity of the mammary tumor-derived cell line C127 is due to the expression of functional microsomal triglyceride transfer protein. *J. Lipid Res.* **42:** 1897–1904.
12. Shelness, G. S., L. Hou, A. S. Ledford, J. S. Parks, and R. B. Weinberg. 2003. Identification of the lipoprotein initiating domain of apolipoprotein B. *J. Biol. Chem.* **278:** 44702–44707.
13. Nolte, R. T. 1994. Structural Analysis of the Human Apolipoproteins: An Integrated Approach Utilizing Physical and Computational Methods. PhD Dissertation. Boston University School of Medicine, Boston, MA.
14. Segrest, J. P., M. K. Jones, V. K. Mishra, G. M. Anantharamaiah, and D. W. Garber. 1994. ApoB-100 has a pentapartite structure composed of three amphipathic alpha-helical domains alternating with two amphipathic beta-strand domains. Detection by the computer program LOCATE. *Arterioscler. Thromb.* **14:** 1674–1685.
15. Ingram, M. F., and G. S. Shelness. 1997. Folding of the amino-terminal domain of apolipoprotein B initiates microsomal triglyceride transfer protein-dependent lipid transfer to nascent very low density lipoprotein. *J. Biol. Chem.* **272:** 10279–10286.
16. Burch, W. L., and H. Herscovitz. 2000. Disulfide bonds are required for folding and secretion of apolipoprotein B regardless of its lipidation state. *J. Biol. Chem.* **275:** 16267–16274.
17. Tran, K., J. Boren, J. Macri, Y. Wang, R. McLeod, R. K. Avramoglu, K. Adeli, and Z. Yao. 1998. Functional analysis of disulfide linkages clustered within the amino terminus of human apolipoprotein B. *J. Biol. Chem.* **273:** 7244–7251.
18. Mann, C. J., T. A. Anderson, J. Read, S. A. Chester, G. B. Harrison, S. Kochl, P. J. Ritchie, P. Bradbury, F. S. Hussain, J. Amey, B. Vanloo, M. Rosseneu, R. Infante, J. M. Hancock, D. G. Levitt, L. J. Banaszak, J. Scott, and C. C. Shoulders. 1999. The structure of vitellogenin provides a molecular model for the assembly and secretion of atherogenic lipoproteins. *J. Mol. Biol.* **285:** 391–408.
19. Segrest, J. P., M. K. Jones, and N. Dashti. 1999. N-terminal domain of apolipoprotein B has structural homology to lipovitellin and microsomal triglyceride transfer protein: a "lipid pocket" model for self-assembly of apoB-containing lipoprotein particles. *J. Lipid Res.* **40:** 1401–1416.
20. Read, J., T. A. Anderson, P. J. Ritchie, B. Vanloo, J. Amey, D. Levitt,

M. Rosseneu, J. Scott, and C. C. Shoulders. 2000. A mechanism of membrane neutral lipid acquisition by the microsomal triglyceride transfer protein. *J. Biol. Chem.* **275:** 30372–30377.
21. Anderson, T. A., D. G. Levitt, and L. J. Banaszak. 1998. The structural basis of lipid interactions in lipovitellin, a soluble lipoprotein. *Structure.* **6:** 895–909.
22. Small, D. M., and D. Atkinson. 1997. The first beta sheet region of apoB(apoB21–41) is a amphipathic ribbon 50–60Å wide and 200Å long which initiates triglyceride binding and assembly of nascent lipoproteins. *Circulation.* **96:** 1.
23. McLeod, R. S., Y. Wang, S. Wang, A. Rusinol, P. Links, and Z. Yao. 1996. Apolipoprotein B sequence requirements for hepatic very low density lipoprotein assembly. Evidence that hydrophobic sequences within apolipoprotein B48 mediate lipid recruitment. *J. Biol. Chem.* **271:** 18445–18455.
24. Liang, J., X. Wu, H. Jiang, M. Zhou, H. Yang, P. Angkeow, L. S. Huang, S. L. Sturley, and H. Ginsberg. 1998. Translocation efficiency, susceptibility to proteasomal degradation, and lipid responsiveness of apolipoprotein B are determined by the presence of beta sheet domains. *J. Biol. Chem.* **273:** 35216–35221.
25. Nolte, R. T., and D. Atkinson. 1992. Conformational analysis of apolipoprotein A-I and E-3 based on primary sequence and circular dichroism. *Biophys. J.* **63:** 1221–1239.
26. White, J. V., C. M. Stultz, and T. F. Smith. 1994. Protein classification by stochastic modeling and optimal filtering of amino-acid sequences. *Math. Biosci.* **119:** 35–75.
27. Schumaker, V. N., M. L. Phillips, and J. E. Chatterton. 1994. Apolipoprotein B and low-density lipoprotein structure: implications for biosynthesis of triglyceride-rich lipoproteins. *Adv. Protein Chem.* **45:** 205–248.
28. Engleman, D. M., T. A. Steitz, and A. Goldman. 1986. Identifying nonpolar transbilayer helices in amino acid sequences of membrane proteins. *Annu. Rev. Biophys. Biophys. Chem.* **15:** 321–353.
29. Nozaki, Y., and C. Tanford. 1971. The solubility of amino acids and two glycine peptides in aqueous ethanol and dioxane solutions. Establishment of a hydrophobicity scale. *J. Biol. Chem.* **246:** 2211–2217.
30. Labourdenne, S., N. Gaudry-Rolland, S. Letellier, M. Lin, A. Cagna, G. Esposito, R. Verger, and C. Rivière. 1994. The oil-drop tensiometer: potential applications for studying the kinetics of (phospho)lipase action. *Chem. Phys. Lipids.* **71:** 163–173.
31. Wang, L., D. Atkinson, and D. M. Small. 2003. Interfacial properties of an amphipathic α-helix consensus peptide of exchangeable apolipoproteins at air/water and oil/water interfaces. *J. Biol. Chem.* **278:** 37480–37491.
32. Adam, N. K. 1941. The Physics and Chemistry of Surfaces. 3rd edition. Oxford University Press, London. 107–115.
33. Benjamins, J., and E. H. Lucassen-Reynders. 1998. Surface dilational rheology of proteins adsorbed at air/water and oil/water interfaces. *In* Proteins at Liquid Interfaces. D. Möbius and R. Miller, editors. Elsevier, Amsterdam. 341–384.
34. Benjamins, J., A. Cagna, and E. H. Lucassen-Reynders. 1996. Viscoelastic properties of triacylglycerol/water interfaces covered by proteins. *Colloids Surf.* **114:** 245–254.
35. Régine, M., D. Lelièvre, and A. Brack. 1999. Surface active properties of amphiphilic sequential isopeptides: comparison between α-helical and β-sheet conformations. *Biopolymers.* **49:** 415–423.
36. Castano, S., B. Desbat, and J. Dufourcq. 2000. Ideally amphipathic β-sheeted peptides at interfaces: structure, orientation, affinities for lipids and hemolytic activity of $(KL)_mK$ peptides. *Biochim. Biophys. Acta.* **1463:** 65–80.
37. Rapaport, H., G. Möller, C. M. Knobler, R. T. Jensen, K. Kjaer, L. Leiserowitz, and D. A. Tirrell. 2002. Assembly of triple-stranded β-sheet peptides at interfaces. *J. Am. Chem. Soc.* **124:** 9342–9343.
38. Rapaport, H., K. Kjaer, T. R. Jensen, L. Leiserowitz, and D. A. Tirrell. 2000. Two-dimensional order in β-sheet peptide monolayers. *J. Am. Chem. Soc.* **122:** 12523–12529.